Lawrence Berkeley National Laboratory

Title
MODULATED MOLECULAR BEAM SCATTERING OF CO AND NO FROM Pt(111) AND THE STEPPED Pt(557) CRYSTAL SURFACES

Permalink
https://escholarship.org/uc/item/1sf1w172

Author
Lin, T.H.

Publication Date
1980-11-01

Lawrence Berkeley Laboratory
UNIVERSITY OF CALIFORNIA

Materials & Molecular Research Division

MODULATED MOLECULAR BEAM SCATTERING OF CO AND NO
FROM Pt(111) AND THE STEPPED Pt(557) CRYSTAL SURFACES

T.H. Lin and G.A. Somorjai

November 1980

DISCLAIMER

MODULATED MOLECULAR BEAM SCATTERING OF CO AND NO FROM Pt(111) AND THE STEPPED Pt(557) CRYSTAL SURFACES

T.H. Lin and G.A. Somorjai

Materials and Molecular Research Division, Lawrence
Berkeley Laboratory, and Department of Chemistry,
University of California, Berkeley, CA 94720

Abstract

The modulated molecular beam scattering of CO and NO from Pt(111) and Pt(557) have been studied in the temperature range of 350-1100 K. For CO scattered from Pt(111), an adsorption-desorption model with constant sticking coefficient fits the data well above 500°K. The best rate parameters are: $\nu = 2.9 \times 10^{13}$, E=29.9 kcal/mole, and S=0.74. For CO scattered from Pt(557) the same model fits the data well above 550°K and the best rate parameters are $\nu = 7.9 \times 10^{13}$, E=33.6 kcal/mole, and S=0.74. The higher activation energy for desorption from the stepped Pt(557), as compared to the flat Pt(111), suggests that while the incident molecules can be adsorbed at the step as well as at the terrace, their desorption energy is influenced by the presence of steps. An adsorption-desorption model with coverage-dependent sticking coefficient fits the data obtained at all temperatures well for both surfaces without change of the kinetic parameters.

For NO scattered from Pt(111), the adsorption-desorption model with constant sticking coefficient fits the data well above 525°K using the rate parameters of $\nu = 6.2 \times 10^{13}$, E=28.6 kcal/mole, and S=0.65. For NO scattered from Pt(557), the same model fits the data well above 525°K with $\nu = 1.2 \times 10^{14}$, E=32.3 kcal/mole, and S=0.71. The higher activation energy suggests again that NO desorption is influenced by the presence of steps.

Below 525°K, the NO scattering results are quite different from those of CO and can not be simulated with the simple models that were tried. The data can be used, however, to rule out several models of surface interactions. NO does not dissociate detectably between 400 K ∿1200 K under our experimental conditions. The sticking coefficient decreases with increasing coverage.

Introduction

Although NO is as important as CO in catalyzed surface reactions, it did not receive as much attention until recently. It is interesting to compare the interactions of NO and CO on platinum single crystal surfaces since they have similar molecular orbital structure, but NO has much lower binding energy (151 kcal/mole as compared to 256 kcal/mole for CO). In this paper we present the results of modulated molecular beam scattering of NO and CO from the flat Pt(111) and the stepped Pt(557) crystal surfaces. The modeling and computational methods to determine surface reaction mechanisms by modulated molecular beam scattering have been derived, and reviewed by other authors (1,2,3).

It is known that CO adsorbs molecularly on low index planes of platinum. The activation energies for desorption from Pt(111) reported are in the range of 24-33 kcal/mole and decrease with increasing coverage (4,5). The sticking coefficients are between 0.6 $\sim$ 0.8 and decrease with increasing coverage (6,7). NO is molecularly adsorbed on platinum surfaces at room temepratures (8-10). The activation energy for desorption is between 20 to 28 kcal/mole (8,10). Partial dissociation of the molecule upon heating has been reported (8,10,11).

Experimental

The apparatus used for the experiment has been described in detail elsewhere (12). Briefly, it consists of three separately pumped chambers as shown in Figure 1. The first diffusion pumped chamber contains the molecular beam source. The second diffusion pumped chamber contains the slotted disk chopper used to modulate the beam in the frequency range of 5 - 200 Hz. The scattering chamber which is pumped by an ion pump and titanium sublimation pump contains the crystal, the rotatable mass spectrometer, and the equipment for Auger electron spectroscopy (AES) and low electron electron diffraction (LEED), and argon ion sputtering. The mass spectrometer AC signal is processed by a phase sensitive lock-in amplifier.

Two crystal surfaces, Pt(111) and Pt(557), were used. The high Miller index surface has six atom wide terraces of (111) orientation

separated by one atom height steps with (100) orientation. The temperature of the crystal was measured by the chromel-alumel thermocouple spot welded to the edge of the crystal. Before any experiment, the crystal was ion sputtered, treated with oxygen, and annealed in situ. The cleanliness was checked by AES.

The molecular beam source backing pressure was 10 Torr for NO unless otherwise noted. Backing pressure was 3 Torr for CO. The incident angle of the beam was 45° and perpendicular to the step in the case of Pt(557). The signal was detected in the integral mode (13). In this mode the mass spectrometer is placed behind the crystal surface and measures the modulated chamber pressure. Each datum was normalized to the hot crystal (1250 K) datum which has a negligible phase lag due to the very short residence time. The normalization takes care of all other causes of phase lag (1) except that due to the surface reaction. Therefore, the normalized data depend on the surface processes only. Between each experimental run the crystal was heated to 1250 K for 3 - 5 minutes to make sure that it was not poisoned during the experiment as a result of adsorption of ambient gases. At the same time, the reference signal was detected that was used for normalization of the data points. In this way any change in the electron multiplier gain, which could be 10% during each day's experiment, was detected and eliminated from the normalized data. At the end of the experiment, the crystal was rechecked with AES.

Results and Discussion

A. CO scattered from Pt(111) and Pt(557) crystal surfaces.

Figures 2(a) and 2(b) show the normalized amplitudes and phase lags as functions of the crystal temperature of CO scattered from Pt(111) at chopping frequencies 10 Hz and 100 Hz, respectively. The solid and dash lines are the theoretical fits to the adsorption-desorption model with coverage-dependent sticking coefficient (see below). The normalized amplitude stays at the value 1.0 at high temperature and drops sharply at lower temperature, then starts to climb at even lower temperature (<500 K). The phase lag is essentially zero at high temperature and has a sharp peak when the amplitude drops sharply. The phase lag stays at zero at

the lowest temperature range where the amplitude is climbing. Note that the pahse lag peak appears at a lower temperature for a chopping frequency of 10 Hz than that for 100 Hz.

To understand how the amplitude and the phase lag vary with crystal temperature, let us consider the adsorption-desorption model with a fixed sticking coefficient s:

$$(1-s)I_0 g(t) \quad \rightarrow \quad A(gas)$$

$$A(gas)$$

$$sI_0 g(t) \longrightarrow A(ads) \overset{k}{\longrightarrow} A(gas)$$
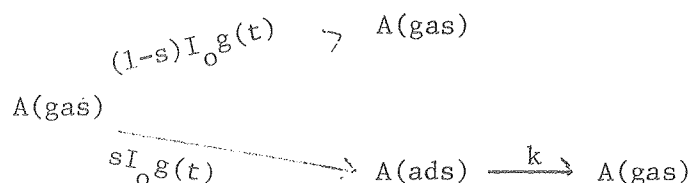
where I_0 is the unmodulated beam intensity, $g(t)$ is the gating function, and $k = \nu e^{-E/RT}$ is the first order Arrhenius desorption rate. Using the method of Jones et al.,(1), it is easy to show that the normalized signal, NS, equals

$$NS = \frac{ks}{k+i\omega} + (1-s) \tag{1}$$

where the first term is due to the fraction of molecules that stick and then desorb from the surface, the second term is contributed by the fraction that does not stick at all. The first term gives rise to the phase lag. The amplitude approaches zero for this term if $k \longrightarrow 0$ due to the long (compared with the chopping frequency) residence time of the molecules that stick, i.e. chemisorb on the surface. Stated differently, the long residence time caused the phase lag as well as the demodulation of the signal. The second term, which may consist of the elastic as well as inelastic scattering, gives rise to no phase lag since the molecule does not stay on the surface long enough. Figure 3 shows how the amplitude and phase lag vary with crystal temperature for this model. At high temperature, $\frac{ks}{k+i\omega} \approx s$ since $k \gg \omega$. At very low temperatures, $\frac{ks}{k+i\omega}$ has negligible amplitude and 90° phase lag since $k \longrightarrow 0$.
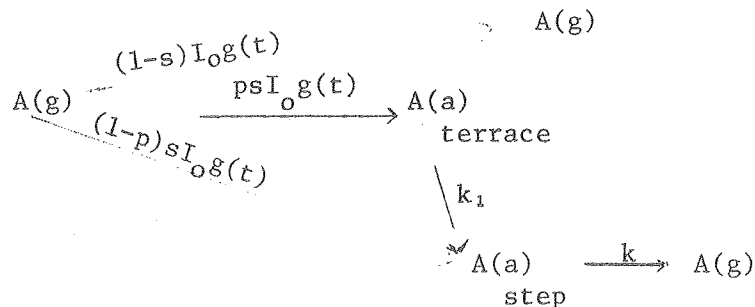
The sum of $\frac{ks}{k+i\omega}$ and $1-s$, however, will have zero phase lag at this very low temperature. Therefore, there will be a temperature where

the phase lag is largest. For a set of fixed ν, E, and s, the phase lag peak position will appear at lower temperature at the smaller chopping frequency, ω.

The adsorption-desorption model with fixed sticking coefficent can explain the general scattering behavior shown in Figure 2, except the rising amplitude at low temperature. A computer least square fit without using the rising amplitude data gives $\nu=2.9\times10^{13}$, $E=29.9$ kcal/mole, and $s=0.737$.

Figures 4(a) and 4(b) show the results of CO scattered from Pt(557). The curves are the theoretical fits to the adsorption-desorption model with coverage dependent sticking coefficient (see below). The general features of the data are the same as that for scattering from Pt(111). For the same chopping frequency, the phase lag peak appears at higher crystal temperature for Pt(557) than that for Pt(111). This indicates that the desorption energy will be higher in the case of Pt(557). The computer fit, without using the rising amplitude data, to the adsorption-desorption model with fixed stick coefficient gives $\nu=7.9\times10^{13}$, $E=33.6$ kcal/mole, and $s=0.74$.

Note that the data show only one binding state of CO for Pt(557) which is a stepped surface and should have at least two states - at the terrace and step site. The higher activation energy suggests that CO desorption occurs from the step site as compared to the terrace site for scattering from Pt(111). Since the sticking coefficients are about the same for both Pt(111) and Pt(557), we believe the molecule can be adsorbed at the step as well as the terrace site and quickly diffuse to the step site before desorption. Therefore, the model for Pt(557) should be

$$
A(g)
$$

$$
A(g) \xrightarrow[\substack{(1-s)I_og(t) \\ (1-p)sI_og(t)}]{psI_og(t)} A(a) \atop \text{terrace}
$$

$$
\Big\downarrow k_1
$$

$$
A(a) \xrightarrow{\ k\ } A(g) \atop \text{step}
$$

where we cannot determine p and k_1 since surface diffusion is not the limiting step.

To explain the rising amplitude at low temperature, we used a coverage dependent sticking coefficient instead of the fixed sticking coefficient. In this new model,

$$s = s_o(1-\theta), \quad \theta = \frac{n}{N}$$

where s_o is the initial sticking coefficient, n is the concentration of CO on the surface, and N is the density of the available site for CO chemisorption. The way of treating this non-linear process has been described by Olander et al,(3). Briefly, by substitution of the functions,

$$n(t) = n_o + n_1 e^{i\omega t} + \ldots$$

$$g(t) = \tfrac{1}{2}(1 + g_1 e^{i\omega t})$$

into the mass balance equation

$$\frac{dn}{dt} = s_o I_o g(t)(1-\theta) - kn$$

we obtain

$$n_o = \frac{s_o I_o}{2}\left(\frac{1}{k + \dfrac{s_o I_o}{2N}}\right)$$

$$n_1 = \frac{s_o I_o}{2} \, g_1 (1 - \frac{n_o}{N}) \frac{1}{i\omega + k\left(\dfrac{s_o I_o}{2N}\right)}$$

The normalized signal, NS, becomes

$$NS = (1-s_o) + s_o(\frac{n_o}{N} + \frac{n_1}{Ng_1}) + k(\frac{n_1}{g_1})\frac{2}{I_o} \tag{2}$$

which has four fitting parameters: s_o, ν, E, and $\frac{I_o}{N}$. The best fit is shown by curves on Figures 2 and 4. The values of the best fitting parameters are, $\nu = 2.1 \times 10^{13}$, $E = 29.5$ kcal/mole, $s_o = 0.732$, $\frac{I_o}{N} = 0.00315$ for Pt(111), and $\nu = 4.3 \times 10^{13}$, $E = 32.8$ kcal/mole, $s_o = 0.726$, $\frac{I_o}{N} = 0.0002$ for Pt(557). It is evident that the values for ν, E, and s_o are almost identical for both models for each surface.

The values of ν, E, and s for both Pt(111) and Pt(557) are in the range of values reported earlier (4-7). The coverage dependent sticking coefficient has also been reported (6,7). The fit between the data and the model is very good for both Pt(111) and Pt(557) except in the low temperature region. Even for Pt(111) we do not expect the simple

function of the coverage dependent sticking coefficient to fit the data well at low temperature. To have a good fit in that region we believe that a more complicated function of the coverage dependent sticking co-efficient has to be chosen.

Note that the adsorbed CO must be highly mobile on Pt(111) since surface diffusion is not the limiting step in our temperature range. H. Ibach et al,(14) pointed out that the preexponential factor can be near 10^{13} for mobile surface species, which is what we find. For Pt(557), the mobility of the adsorbed molecule is reduced due to the presence of the steps. We believe this to be the reason that we obtain a somewhat higher preexponential factor for Pt(557) than that for Pt(111). We find similar structure sensitive behavior for NO scattered from Pt(111) and Pt(557) also as will be shown below.

B.   NO scattered from Pt(111) and Pt(557) crystal surfaces.

Figures 5a, 5b, and 5c show the normalized amplitude and phase lag as a function of the crystal temperature for NO scattered from Pt(111) at 5 Hz, 10 Hz, and 100 Hz chopping frequencies. The curves are the theoretical fit obtained from our model which will be described later. Many features of the phase shift and the amplitude data are quite different from that for CO scattering, especially at 10 Hz and 5 Hz chopping frequencies.
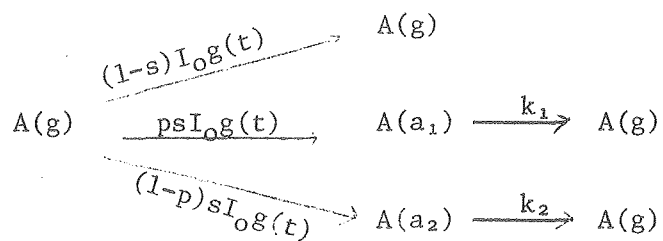
Above 525°K, the data behave like that predicted from an adsorp-tion-desorption model with fixed sticking coefficient. Fitting those data to the model gives $\nu=6.2 \times 10^{13}$, $E=28.6$ kcal/mole, and s=0.645. The activation energy is close to what have been published (8,10) by using TDS. However, previous investigators assumed $\nu=10^{13}$ instead of determining it from experimental data.

Figures 6a and 6b show the results for NO scattering from Pt(557), showing the similar features for Pt(111). Fitting the data above 525°K to the adsorption-desorption model with fixed sticking coefficient gives $\nu=1.2\times10^{14}$, $E=32.3$ kcal/mole, and s=0.79. Comparison of these results with those of Pt(111) suggests that the adsorption-desorption mechanism for NO scattering from Pt(557) at temperatures above 525°K should be the

same as that for CO scattering from the same crystal surface. The adsorbed NO must be highly mobile on Pt(111) at temperatures above 525°K. The preexponential factor is a slightly higher for Pt(557) than that for Pt(111).
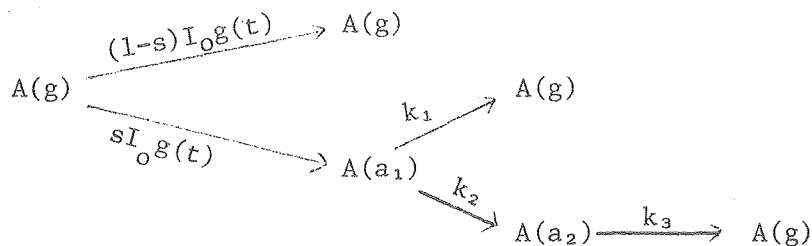
For NO scattering from Pt(111), the data below 525°K are quite different from that predicted from the adsorption-desorption model. With decreasing temperature, the amplitude goes up and then drops sharply. The phase lag changes correspondingly. Below 400°K, the amplitude starts to rise again.

The features of the data can be used to rule out many models immediately. The usual linear, parallel process can explain the characteristics of the phase lag, but not the amplitude. One of the possible models is a modified parallel process--model A,

$$
\begin{array}{c}
A(g) \quad \xrightarrow{(1-s)I_0 g(t)} \quad A(g) \\[2pt]
A(g) \quad \xrightarrow{psI_0 g(t)} \quad A(a_1) \xrightarrow{k_1} A(g) \\[2pt]
\xrightarrow{(1-p)sI_0 g(t)} \quad A(a_2) \xrightarrow{k_2} A(g)
\end{array}
$$

where p is coverage dependent instead of a constant. Basically, we manage the sticking molecule to fill site 1 first before it can migrate to site 2. The curves in Figure 5 are the best fit, without using the data below 400°K, to this model.

Another possible model is as follows, model B,

$$
\begin{array}{c}
A(g) \quad \xrightarrow{(1-s)I_0 g(t)} \quad A(g) \\[4pt]
\qquad \xrightarrow{sI_0 g(t)} \quad A(a_1) \xrightarrow{k_1} A(g) \\[4pt]
\qquad \xrightarrow{k_2} A(a_2) \xrightarrow{k_3} A(g)
\end{array}
$$

The molecule can be adsorbed at site 1 only. It can desorb there or diffuse to another site, 2, before desorbing.

The fits to both models are reasonably good. However, we obtained unusual parameter values for the best fit. For example, $k_2 = 9.8 \times 10^7 e^{-13.3/RT}$

in model A and $k_2 = 9 \times 10^{19} e^{-40.3/RT}$ in model B. Both models were tried to fit the data for NO scattering from Pt(557). The fittings were worse than those for the Pt(111) case and the best fitting parameters are even more difficult to explain. This is not unusual since the surface structure of Pt(557) is more complicated than that of Pt(111).

Note that the unusual result between 450°K - 500°K does not show up in the data obtained using 100 Hz chopping frequency. This means in order to have that new effect, whatever it is, occur, the residence time of the molecule on the surface has to be longer than 0.01 second.

To see how the beam intensity changes the data, we tried NO scattered from Pt(111) at 100 Hz with backing pressure 1.5 Torr instead of 10 Torr and from Pt(557) at 10 Hz with backing pressure of 2 Torr. The results are shown in Figures 7 and 8. The main difference is the sticking coefficient being larger for lower beam intensity. This suggests that the sticking coefficient will decrease as the coverage increases. The same suggestion can be used to explain the rising amplitude below 400°K.

We tried to obtain evidence for NO dissociation by measuring the modulated O_2 and N_2 signals as function of the crystal temperature at different frequencies. Compared with the modulated NO signal, O_2 and N_2 signals were very small and independent of the crystal temperature. We believe NO does not dissociate to any appreciable extent under our experimental conditions.
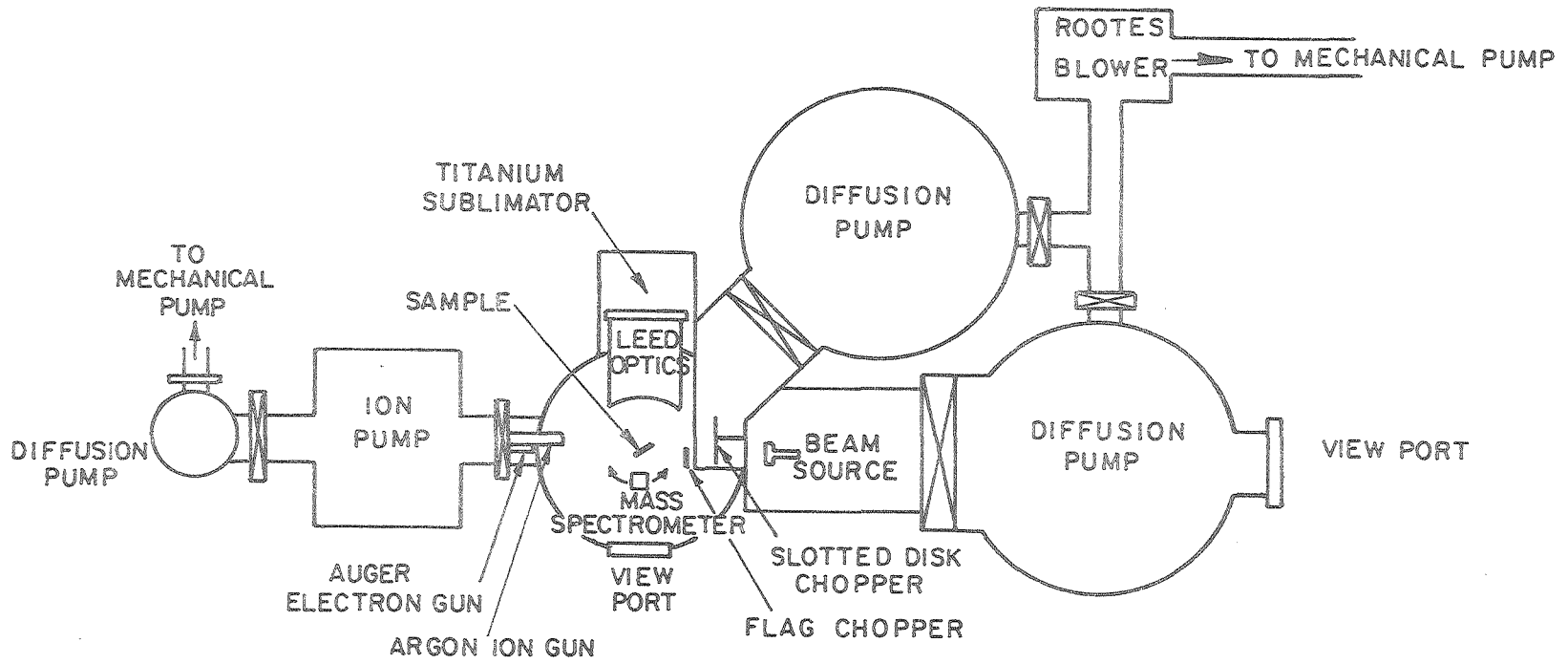
References

1. R.H. Jones, D.R. Olander, W.J. Siekhaus, and J.A. Schwarz, J. Vac. Sci. Technol. 9(1972) 1429.

2. J.A. Schwarz and R.J. Madix, Surface Sci. 46 (1974) 317.

3. D.R. Olander and A. Ullman, Intl. J. Chem. Kin. 8 (1976) 625.

4. G. Ertl, M. Neumann, and K.M. Streit, Surface Sci. 64 (1977) 393.

5. D.M. Collins and W.E. Spicer, Surface Sci. 69 (1977) 85.

6. R.A. Shigeishi and D.A. King, Surface Sci. 58 (1976) 379.

7. G. Ertl, Surface Sci. 89 (1979) 525.

8. C.M. Comrie, W.H. Weinberg, and R.M. Lambert, Surface Sci. 57 (1976) 619.

9. H. Ibach and S. Lehwald, Surface Sci. 76 (1978) 1.

10. J.L. Gland, Surface Sci. 71 (1978) 327.

11. J.L. Gland and B.A. Sexton, Surface Sci. 94 (1980) 355.

12. S.L. Bernasek, Ph.D. Thesis, University of California, Berkeley, 1975.

13. M. Salmeron, R.J. Gale, and G.A. Somorjai, J. Chem. Phys. 67 (1977) 5324.

14. H. Ibach, W. Erley, and H. Wagner, Surface Sci. 92 (1989) 29.

Figure Captions

Figure 1   Schematic diagram of modulated molecular beam scattering apparatus.

Figure 2   Normalized amplitudes and phase lags as function of the crystal
temperature for CO scattered from Pt(111). Curves are theoretical
fits to the   adsorption-desorption model with coverage
dependent sticking coefficient. (a) f=10 hz, (b) f=100 hz.

Figure 3   Amplitude and the phase lag variations as a function of
crystal temperature for the adsorption-desorption model
with fixed sticking coefficient.

Figure 4   Normalized amplitudes and phase lags as a function of the crystal
temperature for CO scattered from Pt(557). Curves are theoretical
fits to the   adsorption-desorption model with coverage de-
pendent sticking coefficient. (a) f=10 hz, (b) f=100 hz.

Figure 5   Normalized amplitudes and phase lags as a function of the crystal
temperature for NO scattered from Pt(111). Curves are theoretical
fits to model A (a) f=5 hz, (b) f=10 hz, and (c) f=100 hz.

Figure 6   Normalized amplitudes and phase lags as a function of the crystal
temperature for NO scattered from Pt(557). Curves are theoretical
fits (a) f=10 hz, (b) f=100 hz.

Figure 7   NO scattered from Pt(111) at 100 hz with backing pressure 1.5
Torr instead of 10 Torr.

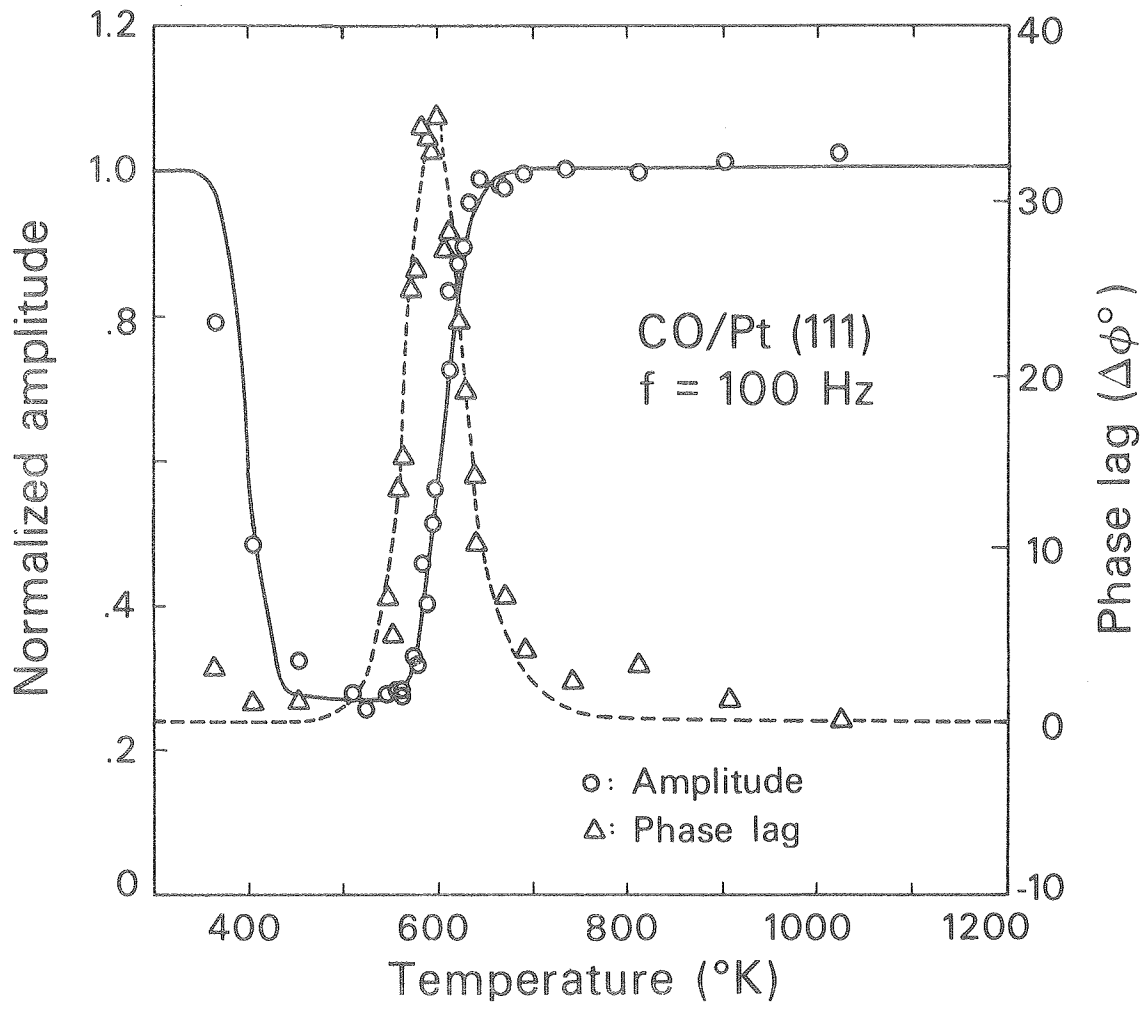Figure 8   NO scattered from Pt(557) at 10 hz with backing pressure 2 Torr
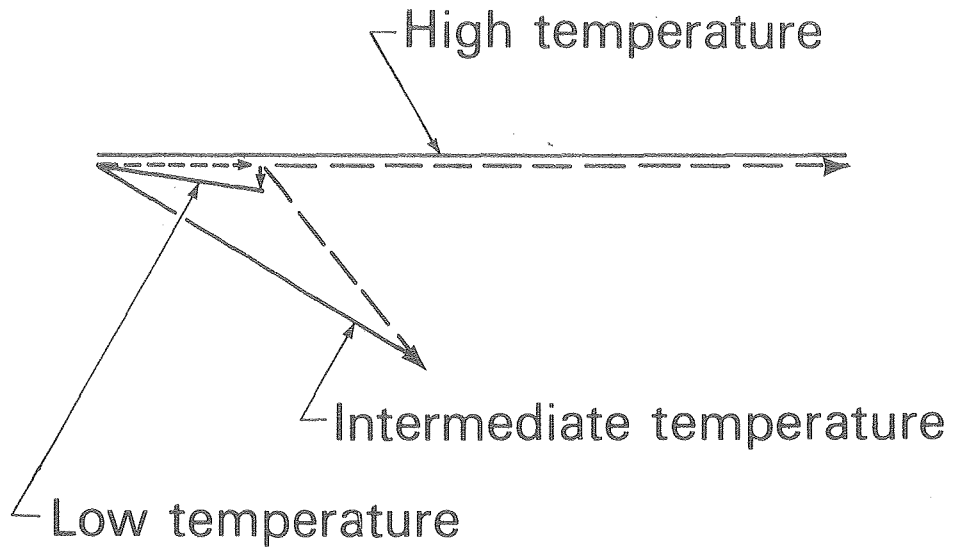instead of 10 Torr.

ROOTES BLOWER → TO MECHANICAL PUMP

TO MECHANICAL PUMP

TITANIUM SUBLIMATOR

SAMPLE

DIFFUSION PUMP

DIFFUSION PUMP

ION PUMP

LEED OPTICS

BEAM SOURCE

DIFFUSION PUMP

VIEW PORT

MASS SPECTROMETER

SLOTTED DISK CHOPPER

AUGER ELECTRON GUN

VIEW PORT

FLAG CHOPPER

ARGON ION GUN

XBL 785-4948

12

Fig. 1

XBL 8011-2325

Fig.2a

CO/Pt (111)
f = 100 Hz

o : Amplitude
△ : Phase lag

XBL 8011-2324

Fig.2b

Fig.3

XBL 8011-2327

Fig.4a

CO/Pt (557)
f = 100 Hz

○ Amplitude
△ Phase lag

Fig.4b

XBL 8011-2326

Fig.5a

NO/Pt (111)
f = 10 Hz
Model A

o Amplitude
△ Phase lag

XBL 8011-2329

Fig.5b

NO/Pt (111)
f = 100 Hz
Model A

o Amplitude
△ Phase lag
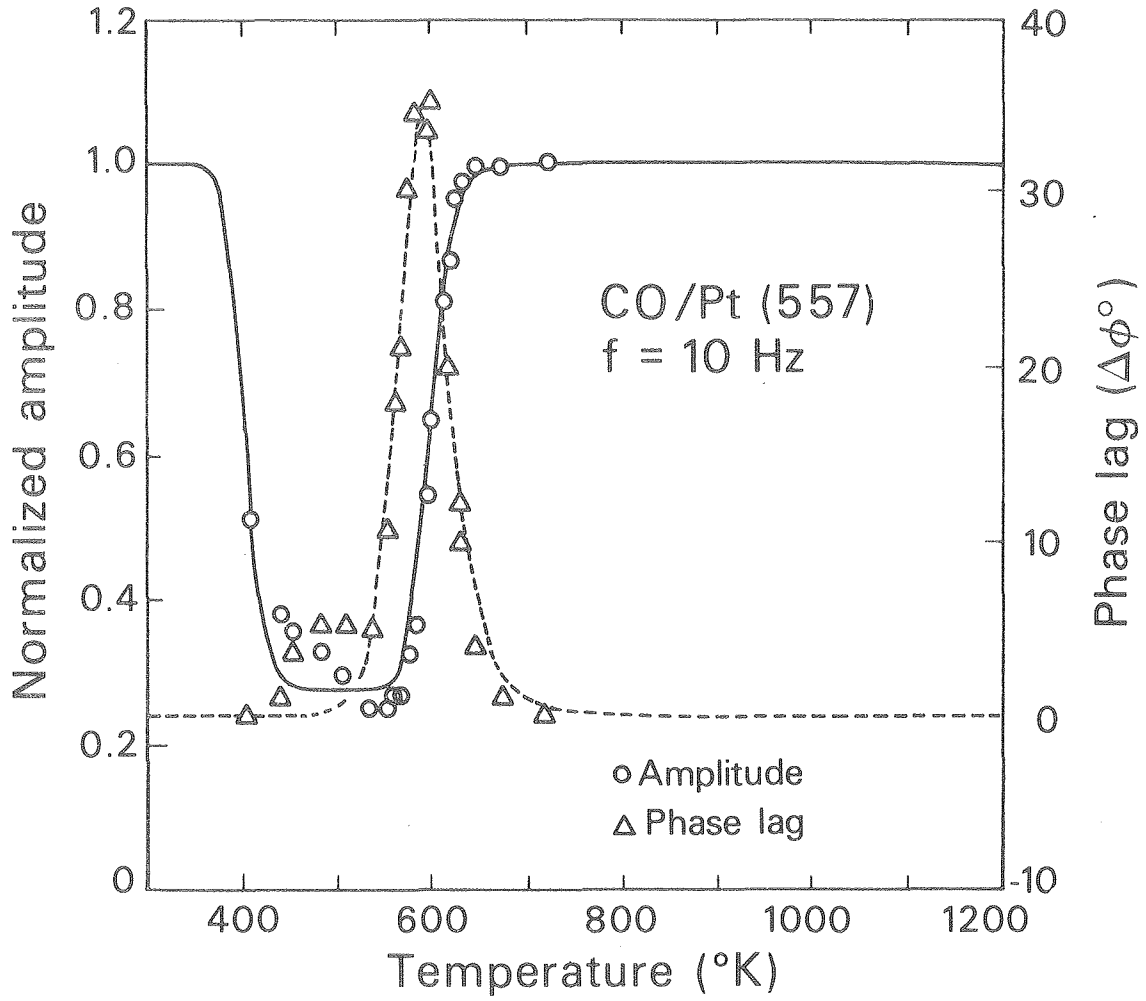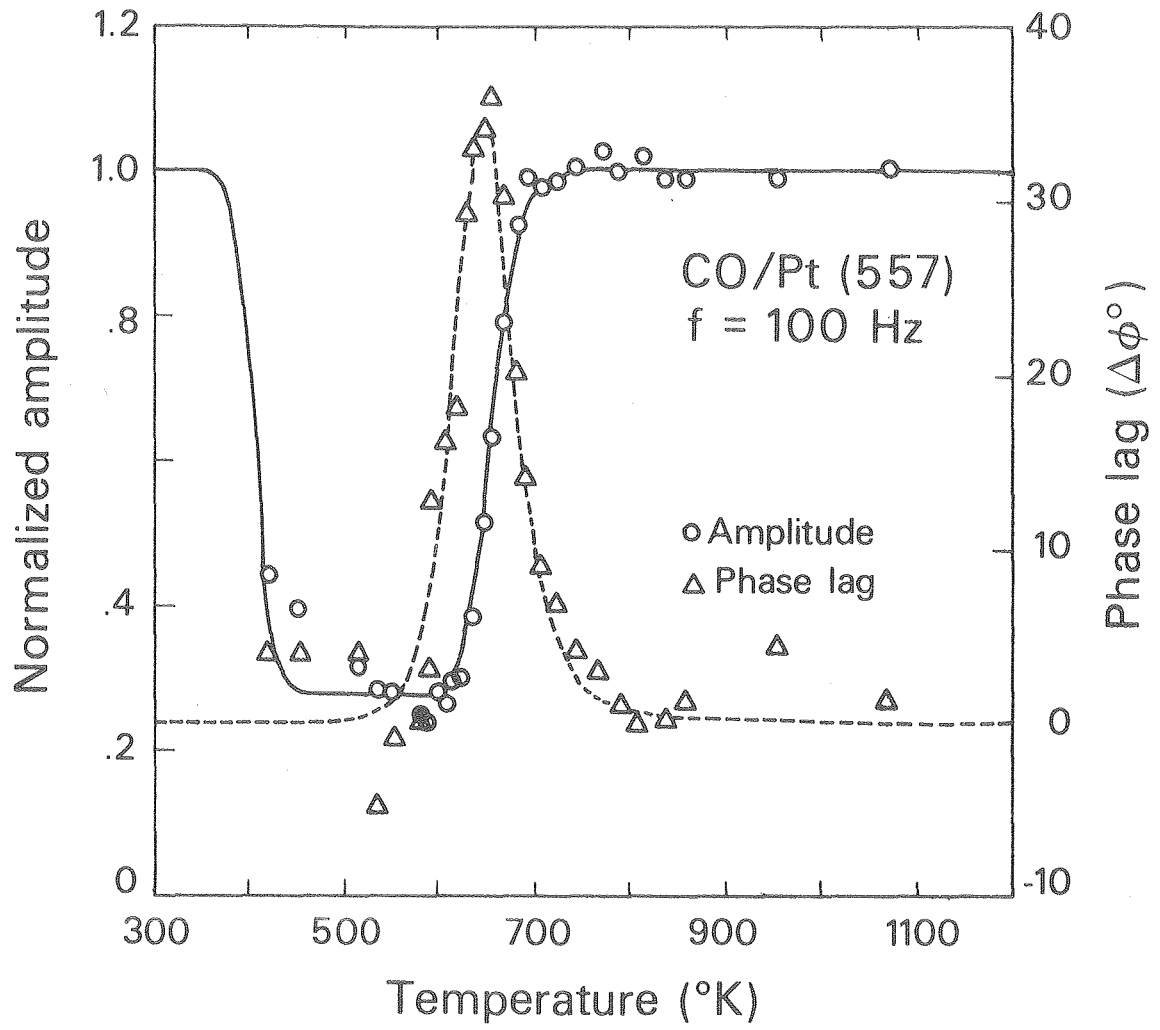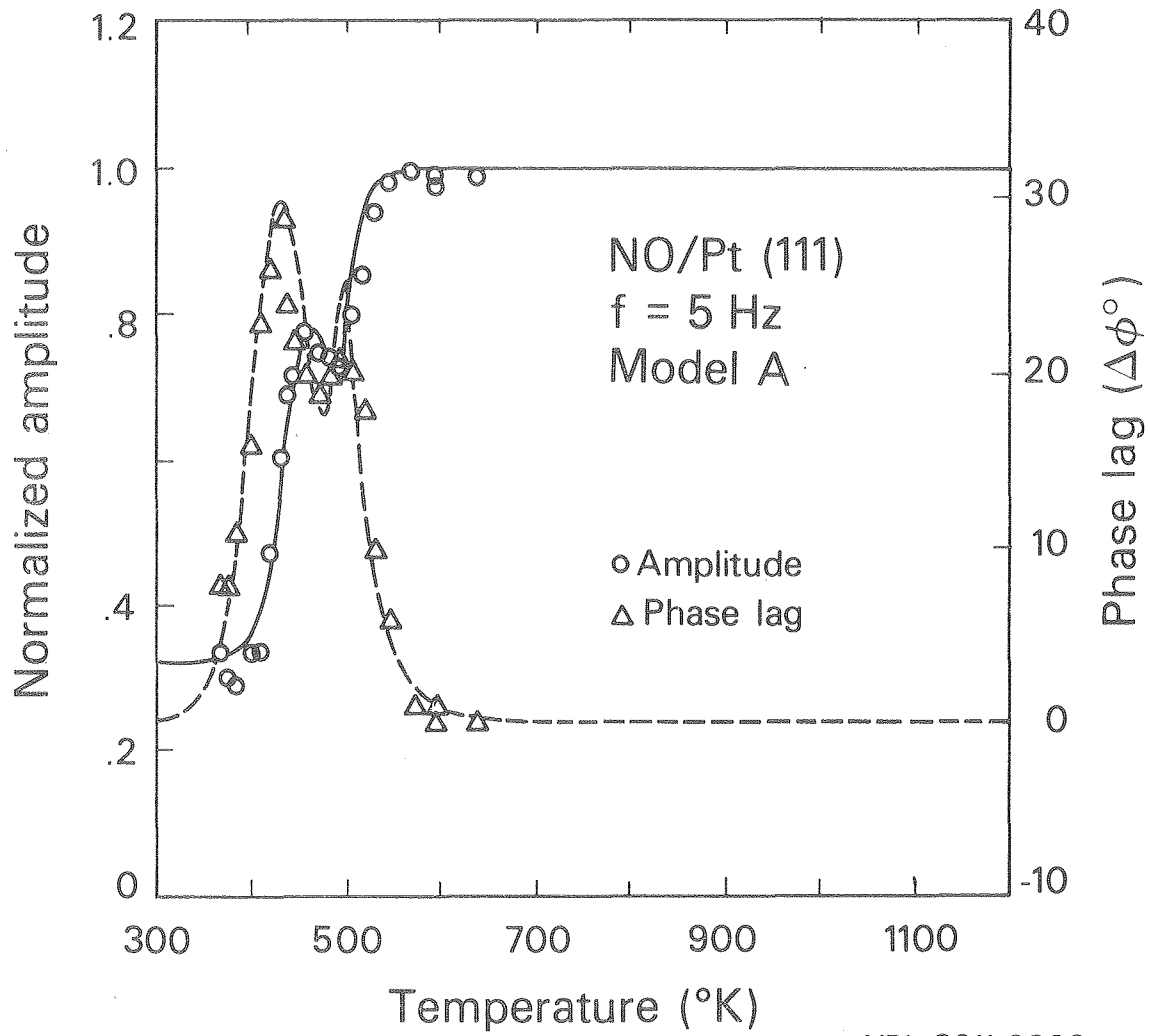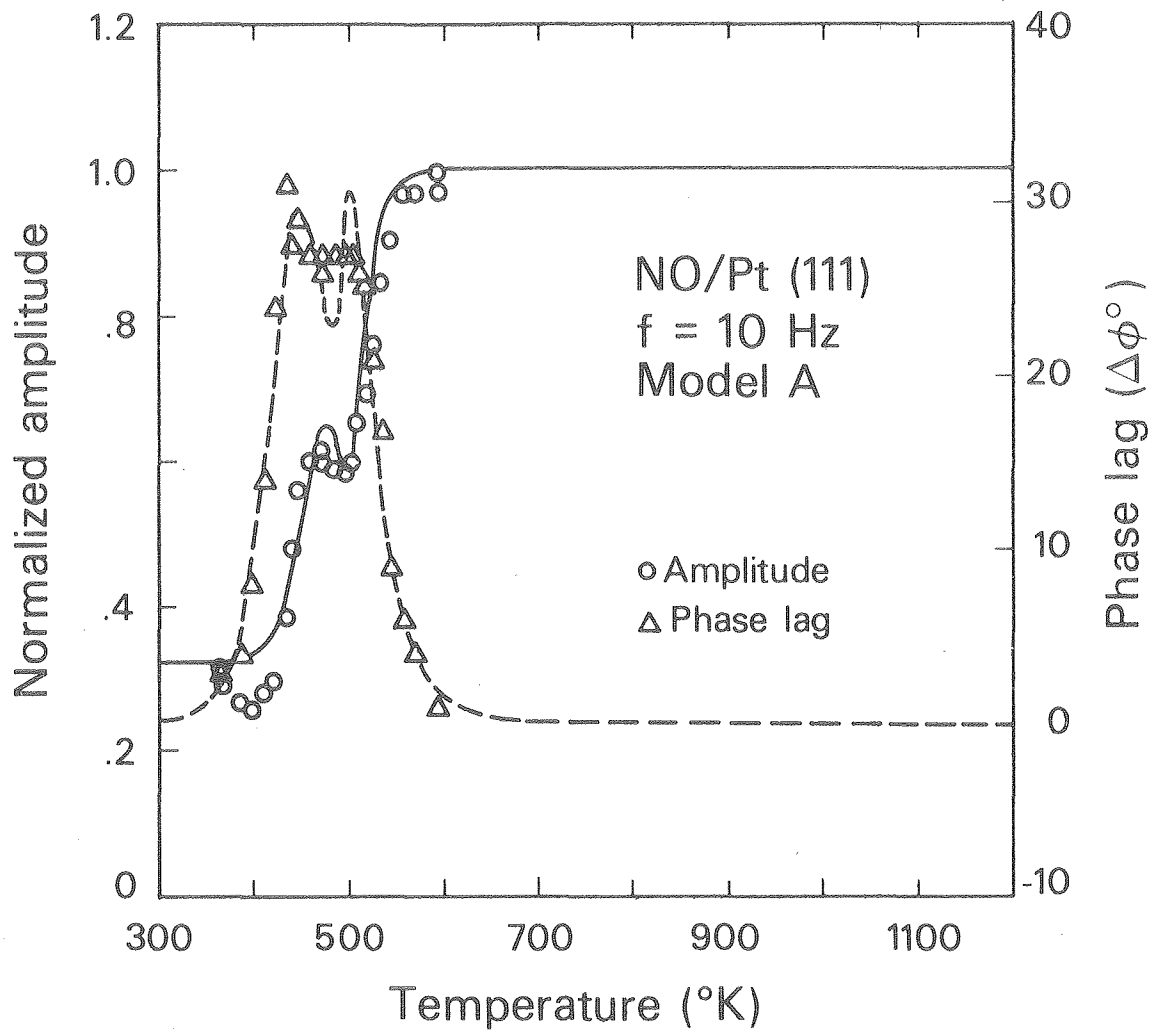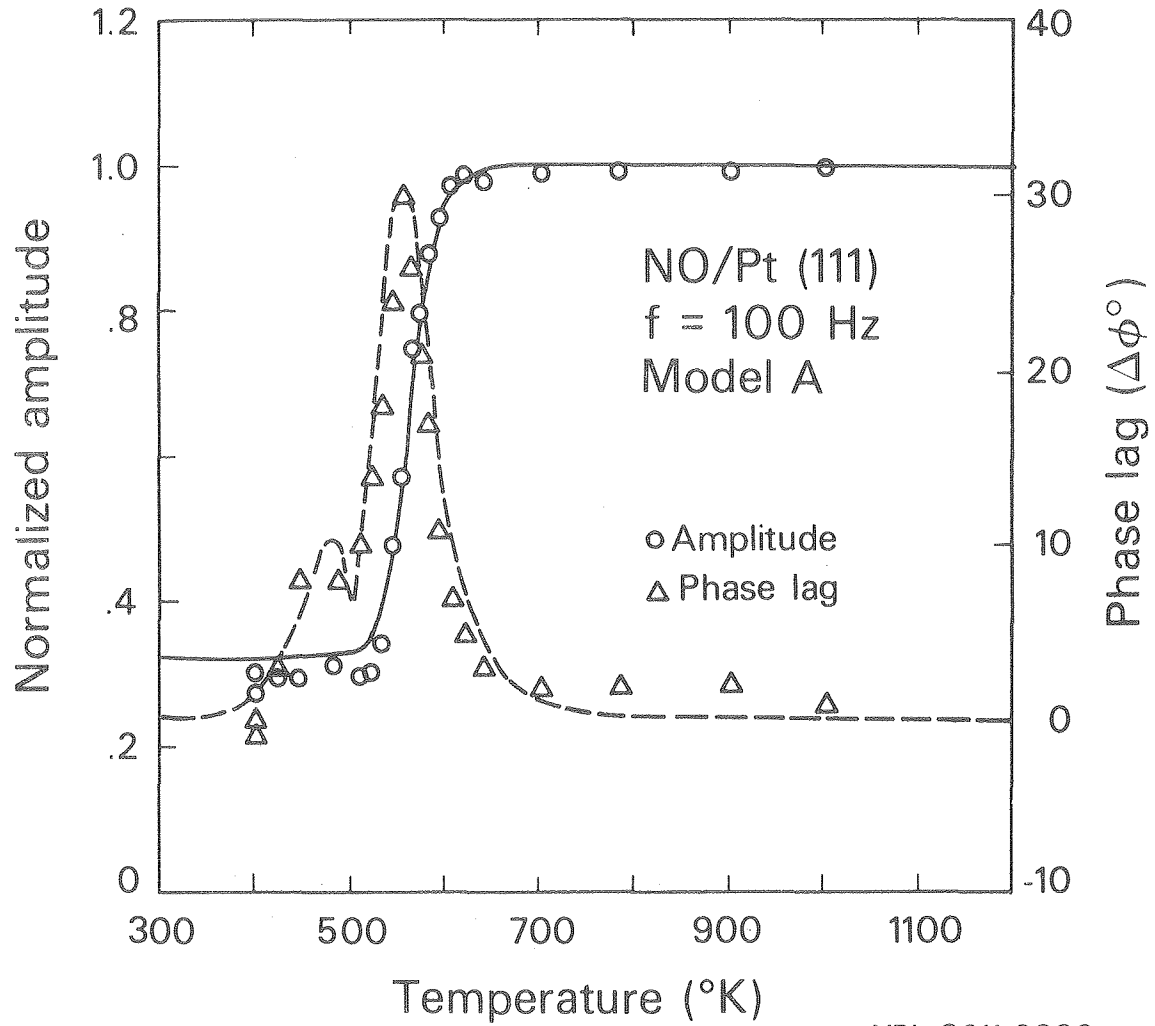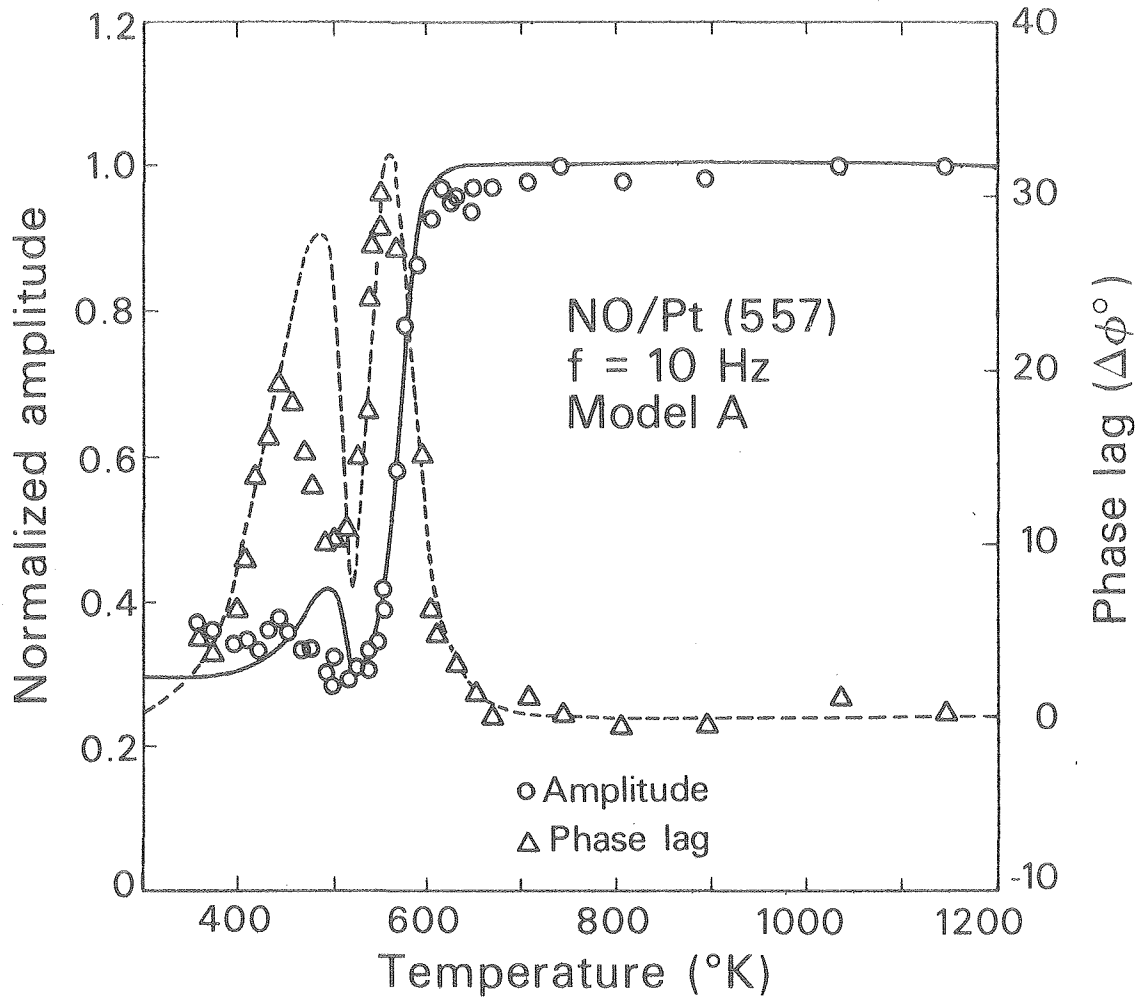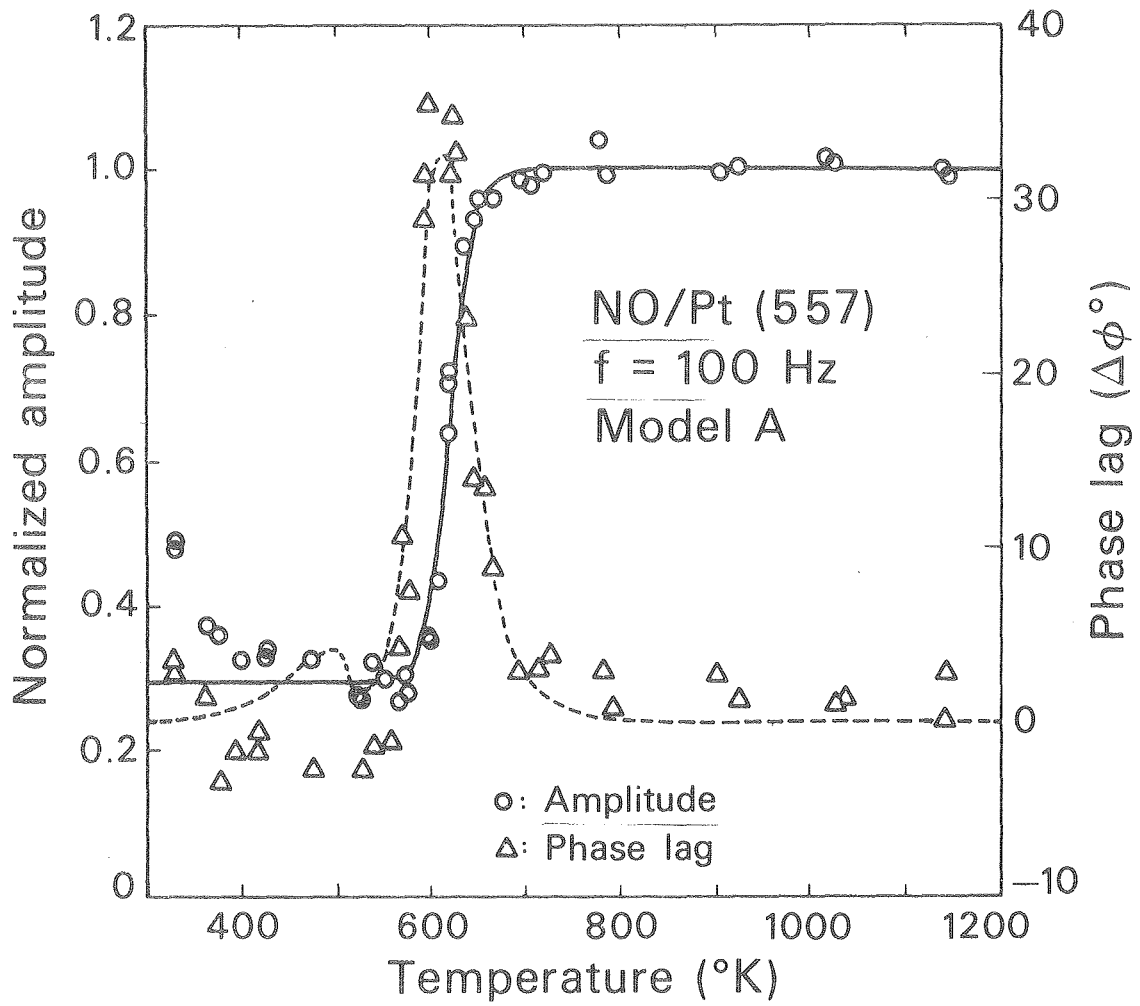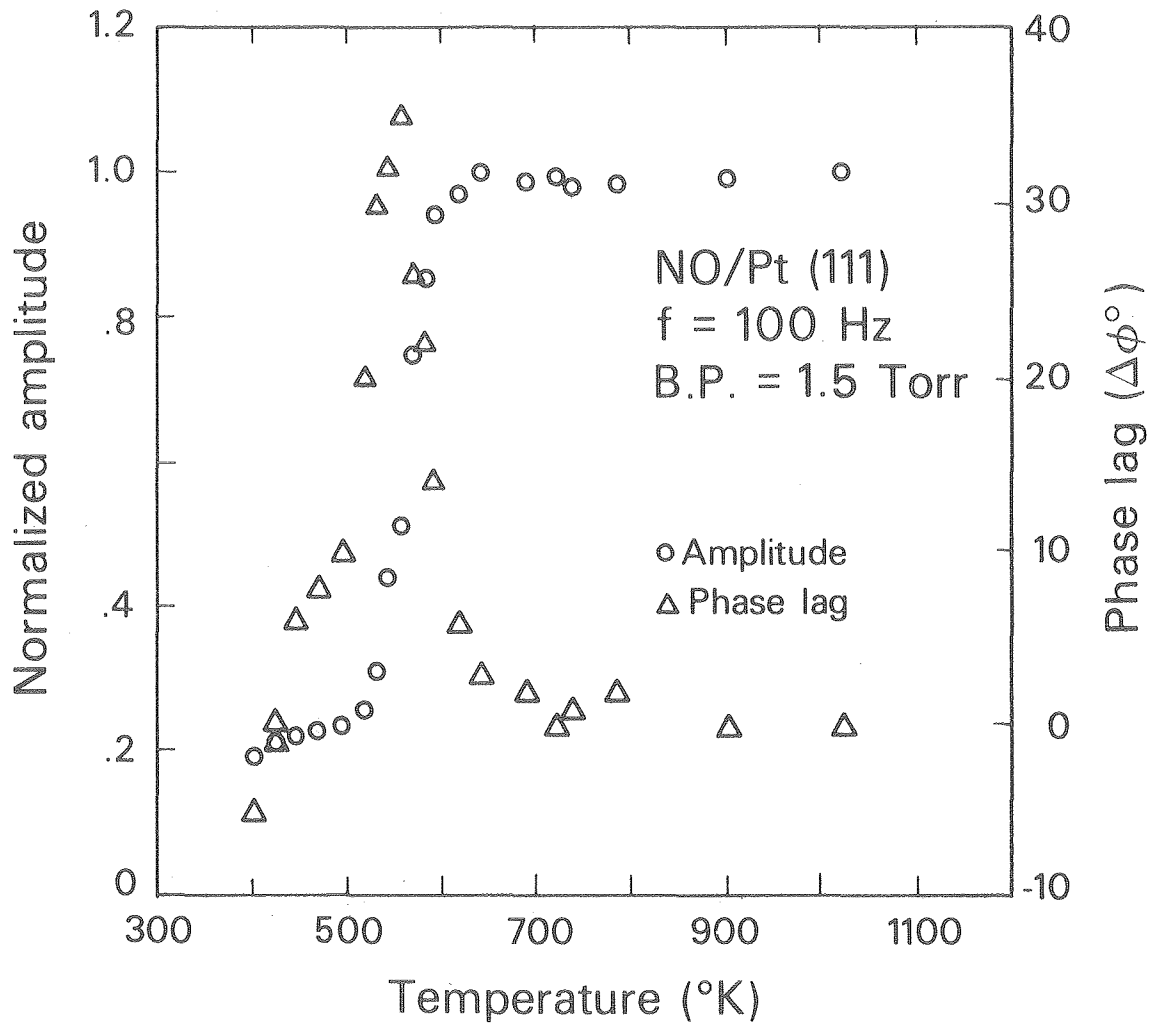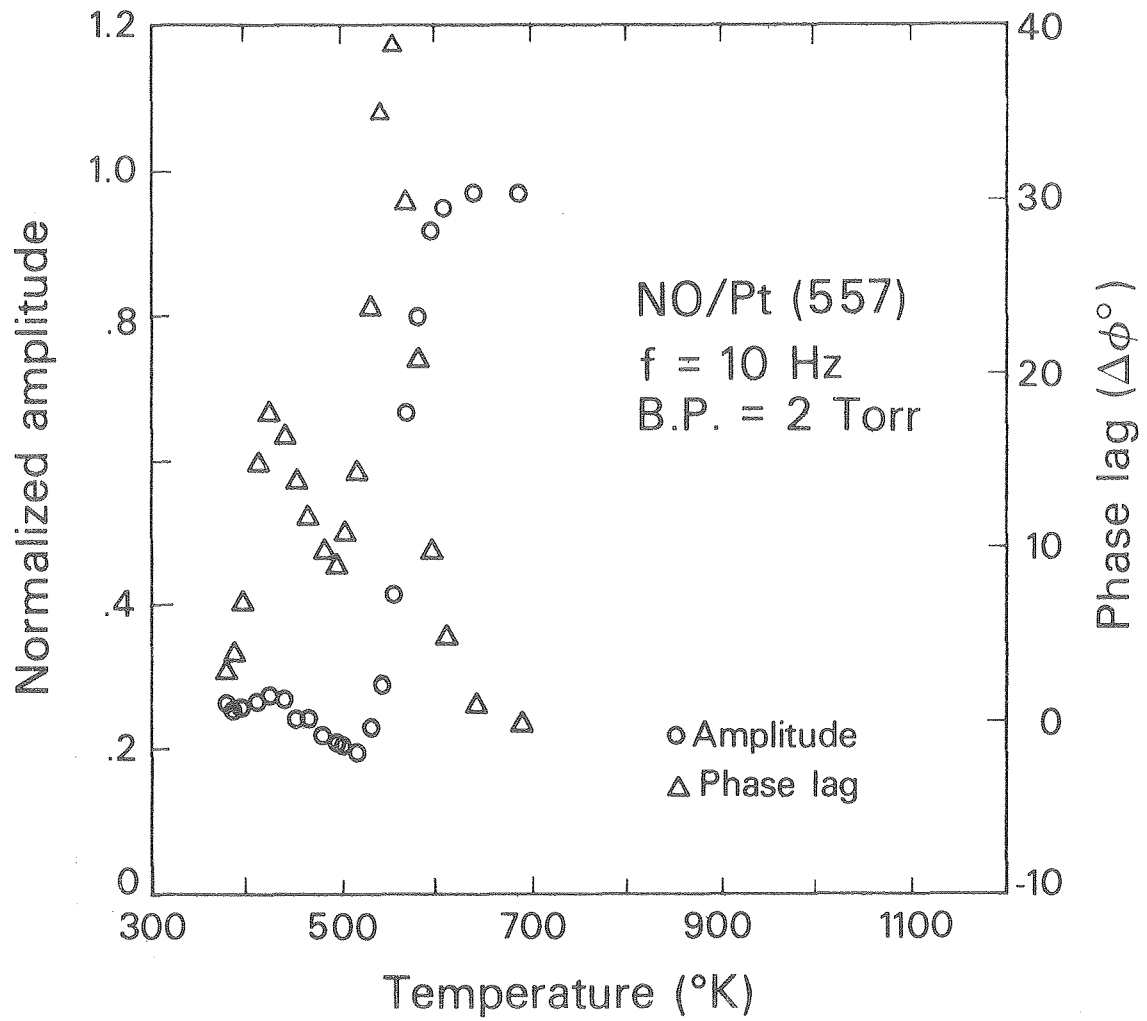
XBL 8011-2332

Fig.5c

XBL 8011-2322

Fig.6a

XBL 8011-2323

Fig.6b

Fig.7

XBL 8011-2330

Fig.8